# Observation de l'horizon des événements situé à la frontière du trou noir supermassif de la galaxie M87 (Messier 87 = NGC 4486)

Denis Gilbert, physicien
www.denisgilbert.com
@dgscientifik

Présenté au Club d'astronomie de Rimouski
2019-04-12

# Shep Doeleman, directeur du EHT

## Conférence de presse du 10 avril 2019

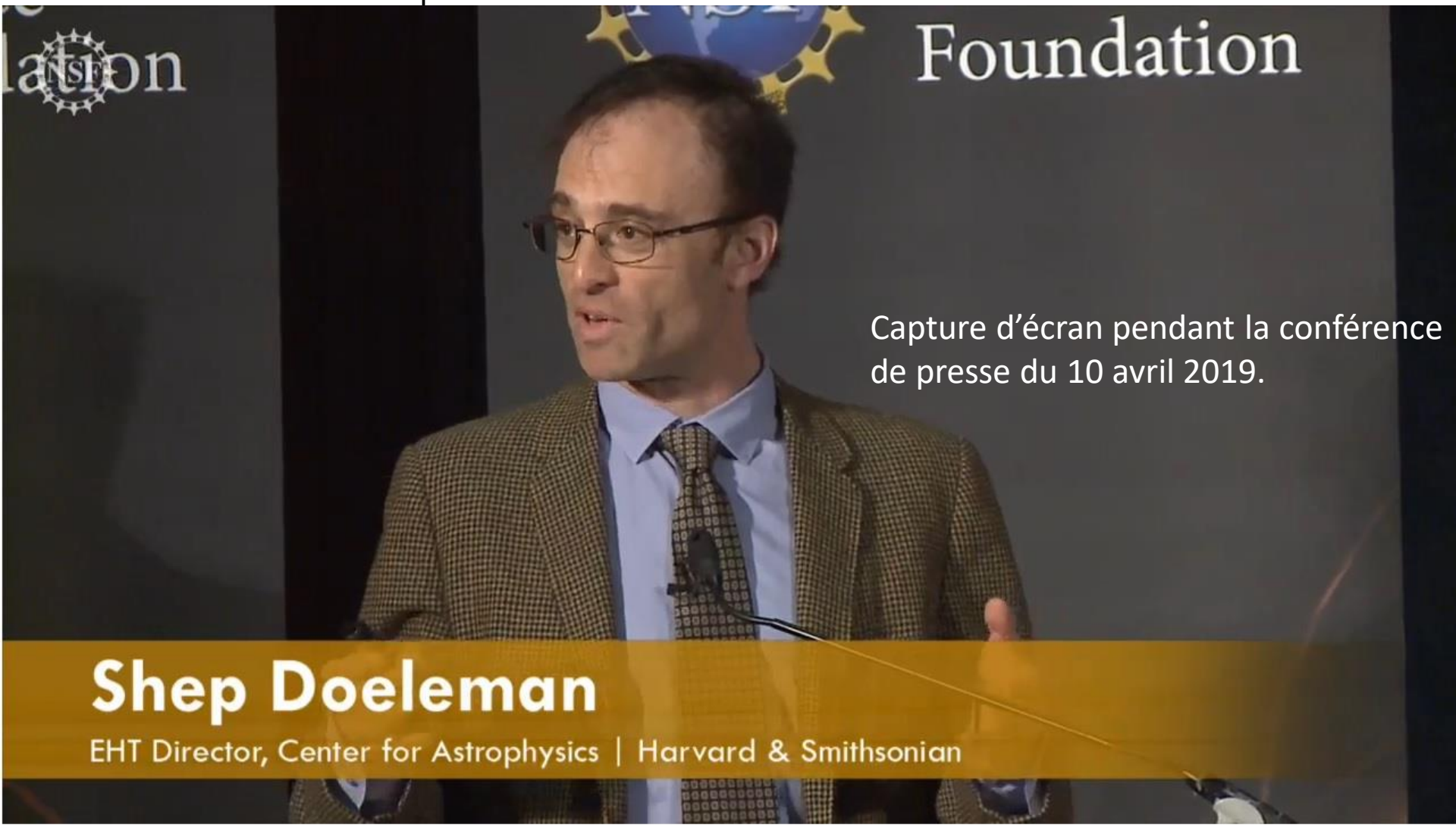


Capture d'écran pendant la conférence de presse du 10 avril 2019.

National Science Foundation/Event Horizon Telescope press conference

https://iopscience.iop.org/journal/2041-8205/page/Focus_on_EHT

# Liens vers six articles publiés dans "The Astrophysical Journal Letters"

**First M87 Event Horizon Telescope Results**:

1. The Shadow of the Supermassive Black Hole
2. Array and Instrumentation
3. Data Processing and Calibration
4. Imaging the Central Supermassive Black Hole
5. Physical Origin of the Asymmetric Ring
6. The Shadow and Mass of the Central Black Hole

# Configuration du EHT en avril 2017

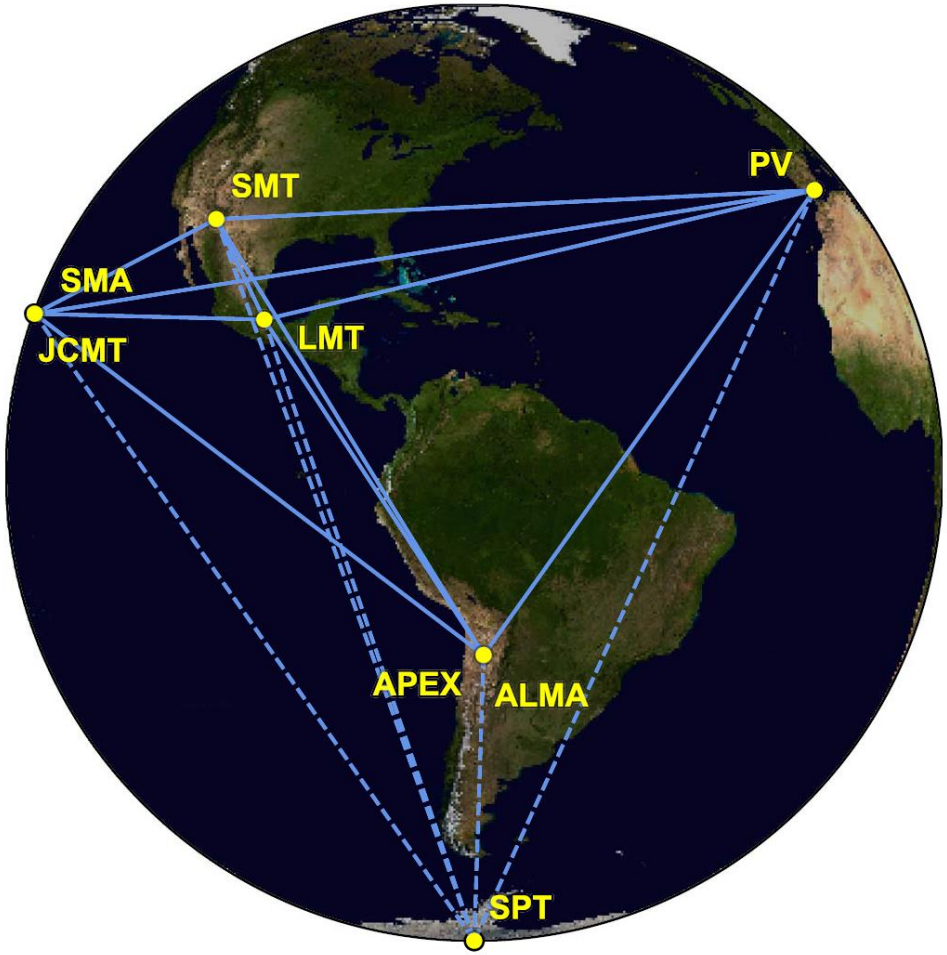


**Figure 1.** Eight stations of the EHT 2017 campaign over six geographic locations as viewed from the equatorial plane. Solid baselines represent mutual visibility on M87* (+12° declination). The dashed baselines were used for the calibration source 3C279 (see Papers III and IV).

Article # 1

# Huit radiotélescopes constituant le EHT

The radio telescope observatories involved in Event Horizon Telescope's observations were (clockwise from top left): Atacama Large Millimeter/submillimeter Array (ALMA) in Chile; SubMillimeter Array (SMA) in Hawaii; South Pole Telescope (SPT) in Antarctica; Submillimeter Telescope (SMT) in Arizona; Atacama Pathfinder Experiment (APEX) in Chile; Large Millimeter Telescope (LMT) in Mexico; James Clerk Maxwell Telescope (JCMT) in Hawaii; and Institut de Radioastronomie Millimétrique (IRAM 30m) in Spain.

# Fonctionnement du EHT

En synchronisant les 8 radiotélescopes du EHT, on obtient un télescope avec un diamètre équivalent à celui de la planète Terre.
VLBI = Very Large Baseline Interferometry

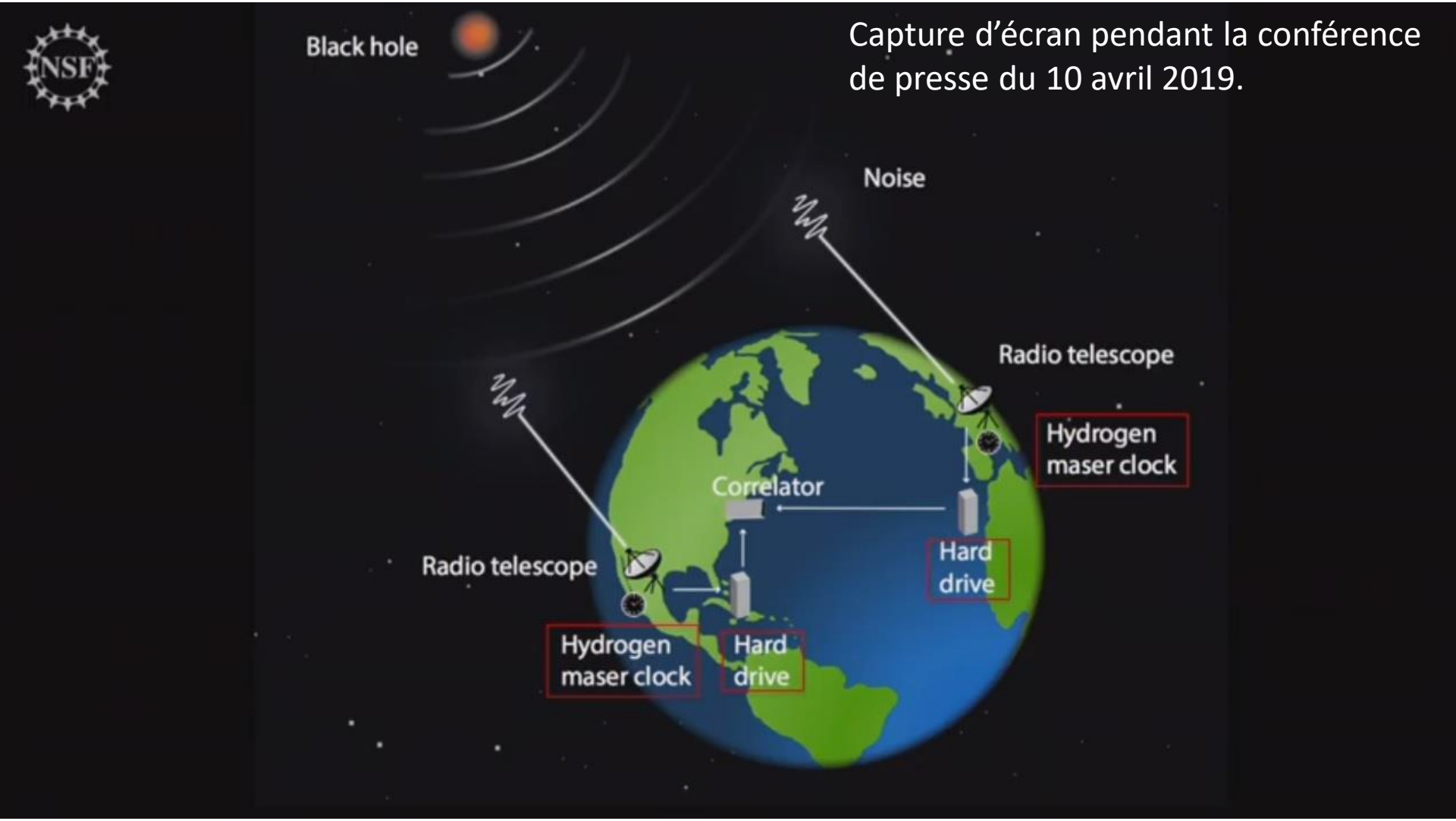


Capture d'écran pendant la conférence de presse du 10 avril 2019.

# Résolution angulaire du EHT

- 20 μas (20 / 360 / 60 / 60 / 1,000,000 degré)
- 2000 fois plus fine que celle de Hubble
- Permet de voir une balle de golf à la surface de la Lune.
- Permet de lire un article du New York Times dans Central Park à partir de Paris

# Données astronomiques prises en compte au moment de la conception technique du EHT



**Table 1**
Assumed Physical Properties of Sgr A* and M87 Used to Establish Technical Goals[a]

| | | Sgr A* | M87 |
|---|---|---|---|
| Black Hole Mass | $M$ ($M_\odot$) | $4.1 \times 10^6$ (1) | $(3.3–6.2) \times 10^9$ (5), (6) |
| Distance | $D$ (pc) | $8.34 \times 10^3$ (2) | $16.8 \times 10^6$ (7) |
| Schwarzschild Radius | $R_s$ ($\mu$as) | 9.7 | 3.9–7.3 |
| Shadow Diameter[b] | $D_{sh}$ ($\mu$as) | 47–50 | 19–38 |
| Brightness Temperature[c] | $T_B$ (K) | $3 \times 10^9$ (3) | $10^{10}$ (8) |
| Period ISCO[d] | $P_{ISCO}$ | 4–54 minutes | 2.4–57.7 days |
| Mass Accretion Rate[e] | $\dot{M}$ ($M_\odot$ yr$^{-1}$) | $10^{-9}$–$10^{-7}$ (4) | $<10^{-3}$ (9) |

**Notes.**
[a] Sgr A*: $\alpha_{J2000.0} = 17^h45^m40^s.0409$, $\delta_{J2000.0} = -29°00'28''.118$ (10); M87: $\alpha_{J2000.0} = 12^h30^m49^s.4234$, $\delta_{J2000.0} = 12°23'28''.044$ (11).
[b] The shadow diameter is within the range 4.8–5.2 $R_s$ depending on black hole spin and orientation to the observer's line of sight (Johannsen & Psaltis 2010).
[c] Brightness temperatures are reported for an observing frequency of 230 GHz.
[d] $P_{ISCO}$ range is given in the case of maximum spin for both prograde (shortest) and retrograde (longest) orbits (Bardeen et al. 1972).
[e] Mass accretion rates $\dot{M}$ are estimated from measurements of Faraday rotation imparted by material in the accretion flow around the black hole.
**References.** (1) GRAVITY Collaboration et al. (2018a), (2) Reid et al. (2014), (3) Lu et al. (2018), (4) Marrone et al. (2007), (5) Walsh et al. (2013), (6) Gebhardt et al. (2011), (7) Blakeslee et al. (2009), EHT Collaboration et al. (2019e), (8) Akiyama et al. (2015), (9) Kuo et al. (2014), (10) Reid & Brunthaler (2004), (11) Lambert & Gontier (2009).

Article # 2

# Photo de M87 par le télescope Hubble

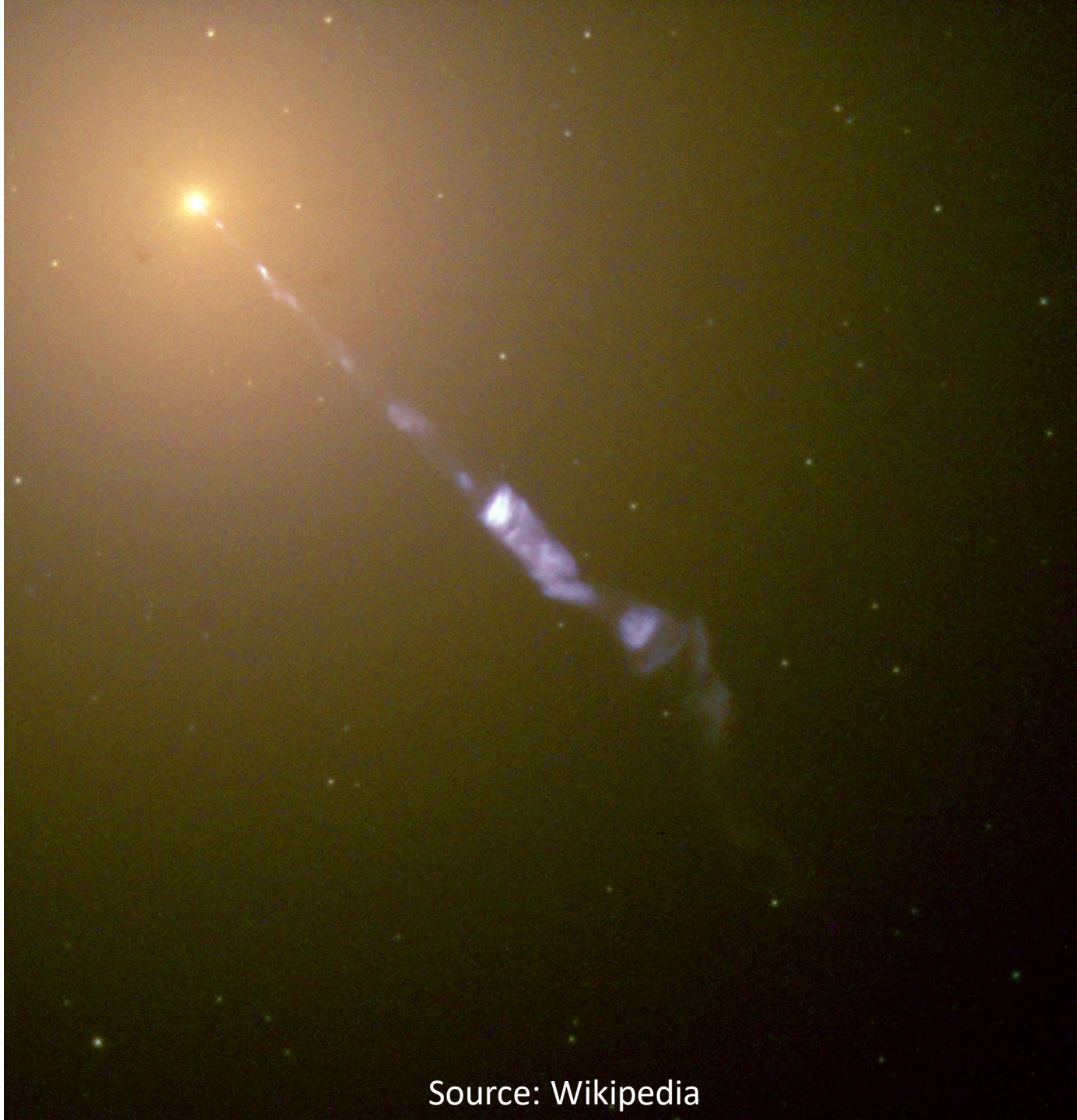

Source: Wikipedia

# Ondes radio émises par le plasma surchauffé (milliards de °C) près de la frontière du trou noir supermassif de M87 (NGC 4486)

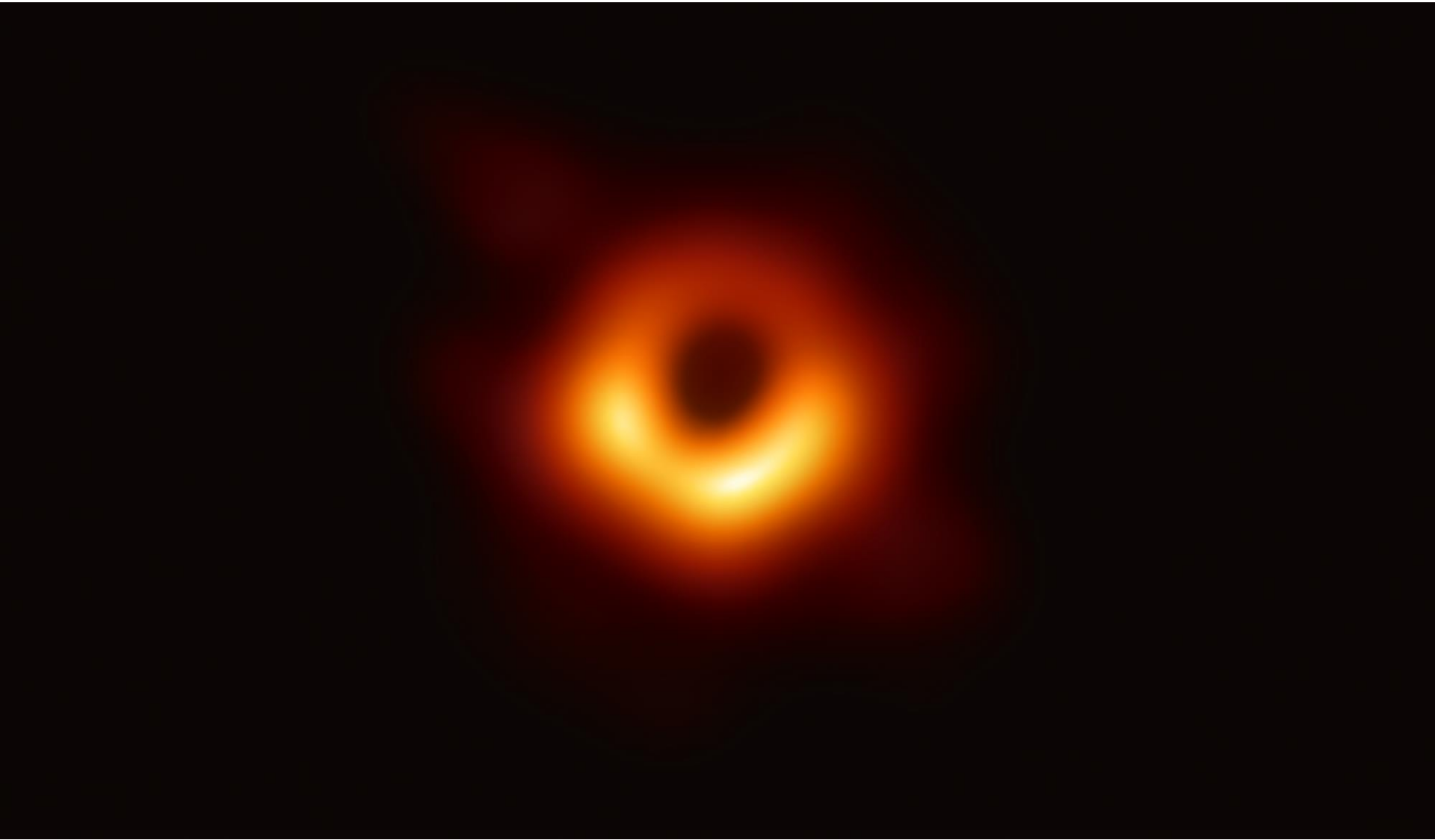

SIZE COMPARISON:

# THE M87 BLACK HOLE AND OUR SOLAR SYSTEM

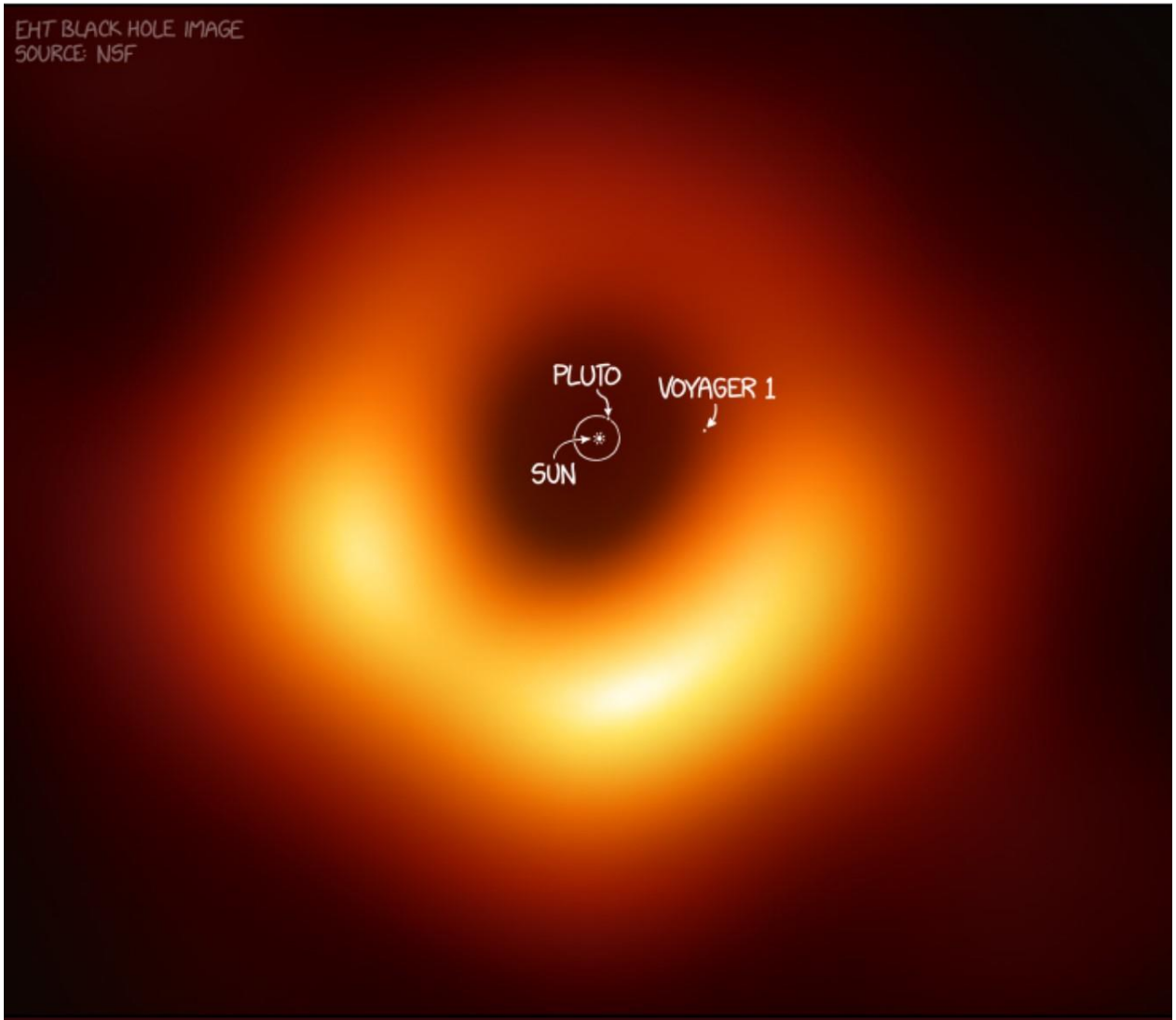

# Anatomie d'un trou noir

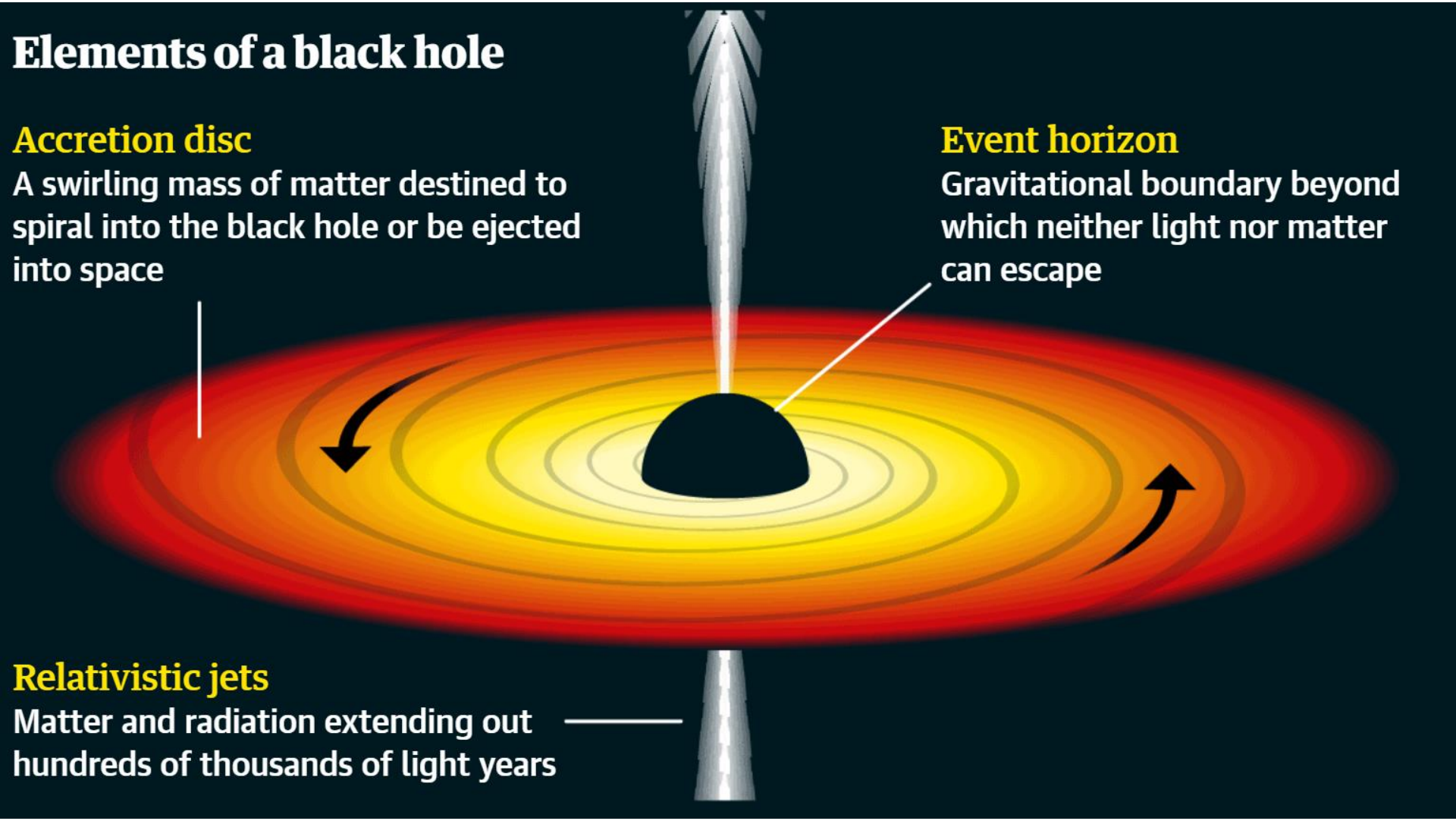


https://www.theguardian.com/science/2019/apr/10/black-hole-picture-captured-for-first-time-in-space-breakthrough

# EHT = Event Horizon Telescope
# Télescope d'horizon des événements

- L'horizon des événements est la frontière externe du trou noir.
- Nous voyons les ondes électromagnétiques émises par la matière surchauffée (plasma). Les ondes qui frôlent l'horizon des événements sont les plus brillantes.
- Nous ne pouvons pas voir le trou noir comme tel, mais nous pouvons détecter son ombre située au centre de l'image.

# Qu’est que nous montre l’image?

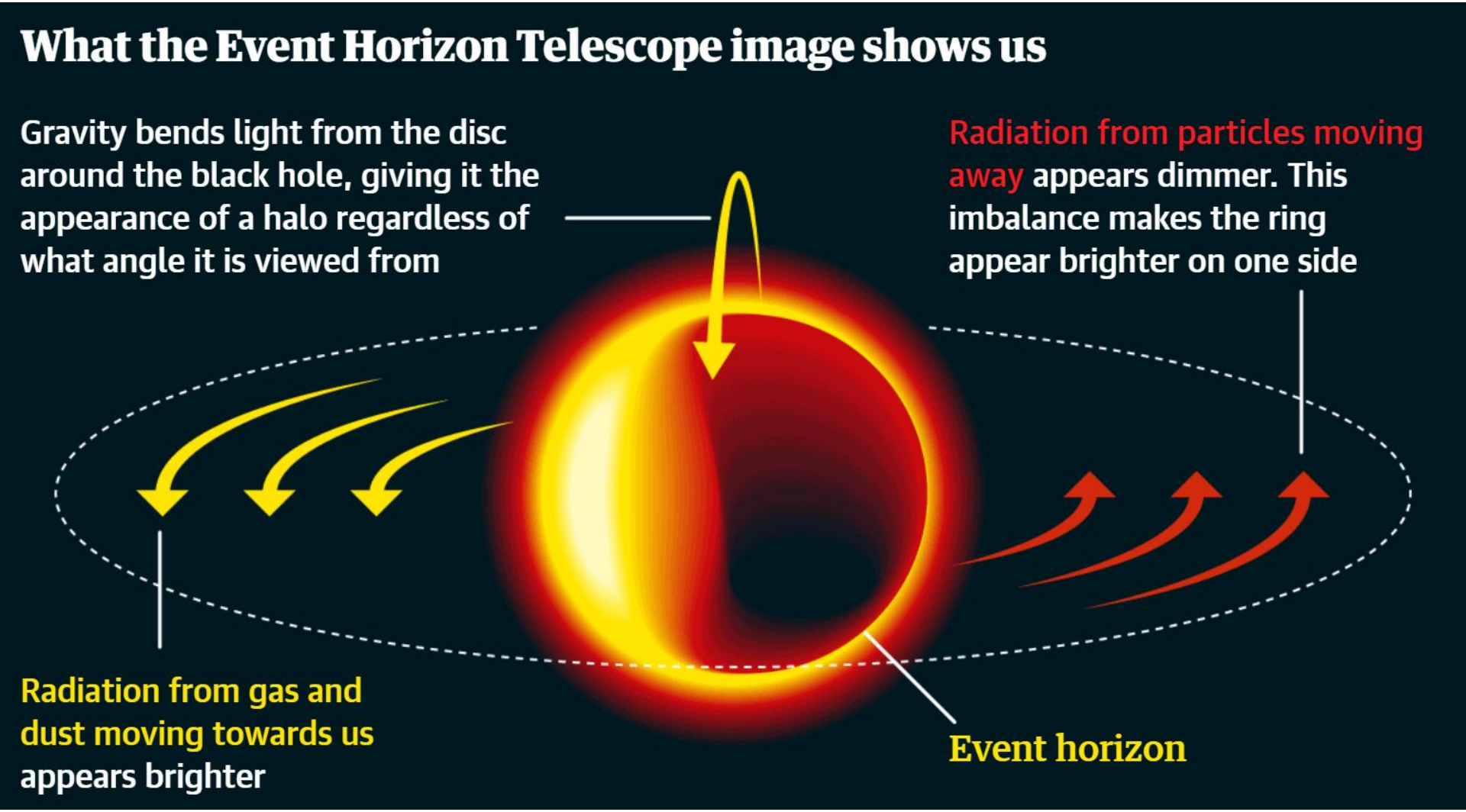


https://www.theguardian.com/science/2019/apr/10/black-hole-picture-captured-for-first-time-in-space-breakthrough

# Horaire des 4 journées d'observation de la galaxia Messier 87 et du quasar 3C279 pour la calibration des données



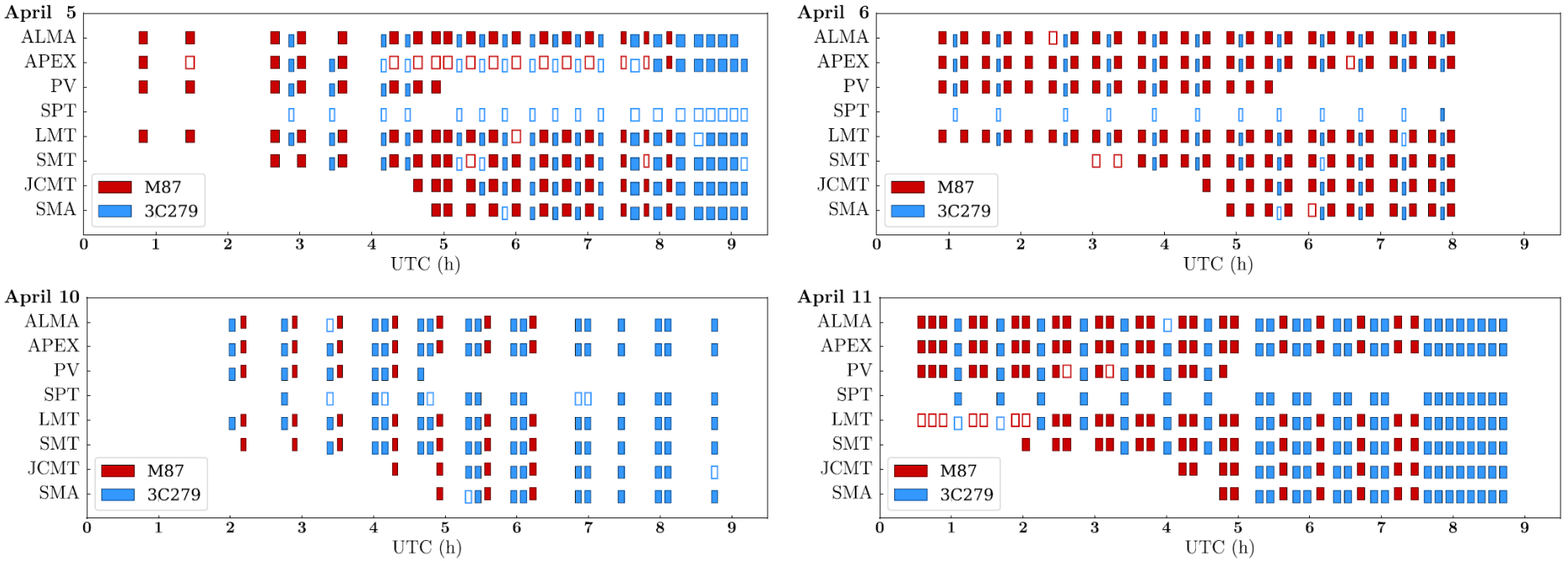


**Figure 2.** EHT 2017 observing schedules for M87 and 3C 279 covering the four days of observations. Empty rectangles represent scans that were scheduled, but were not observed successfully due to weather, insufficient sensitivity, or technical issues. The filled rectangles represent scans corresponding to detections available in the final data set. Scan duration varies between 3 and 7 minutes, as reflected by the width of each rectangle.

Article # 3

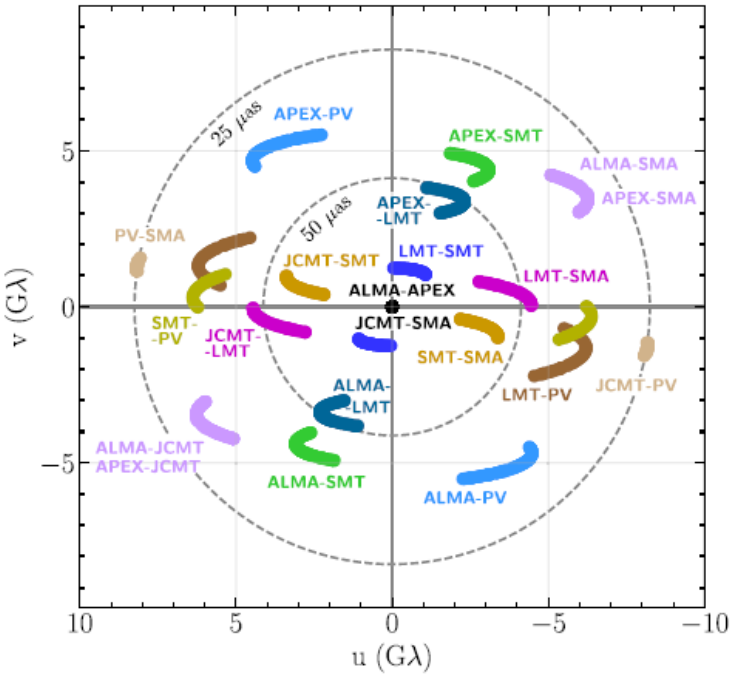


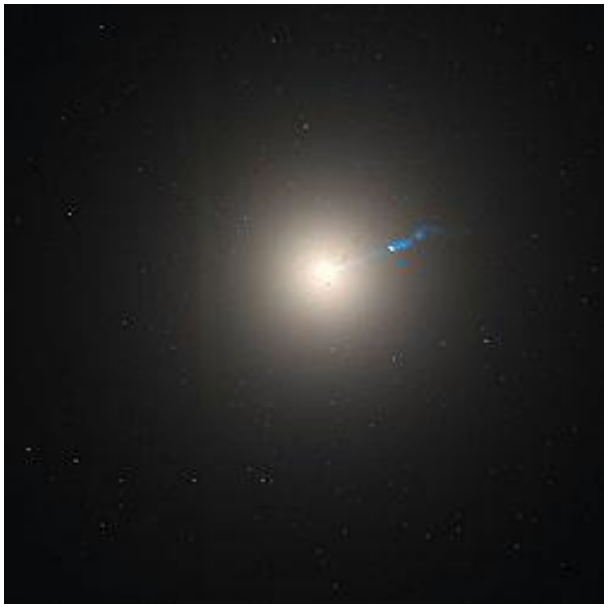

M87

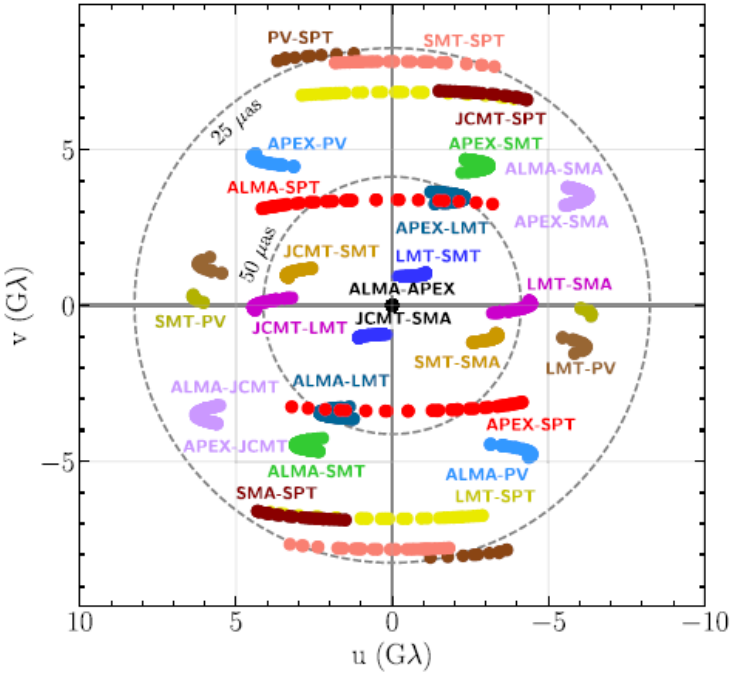


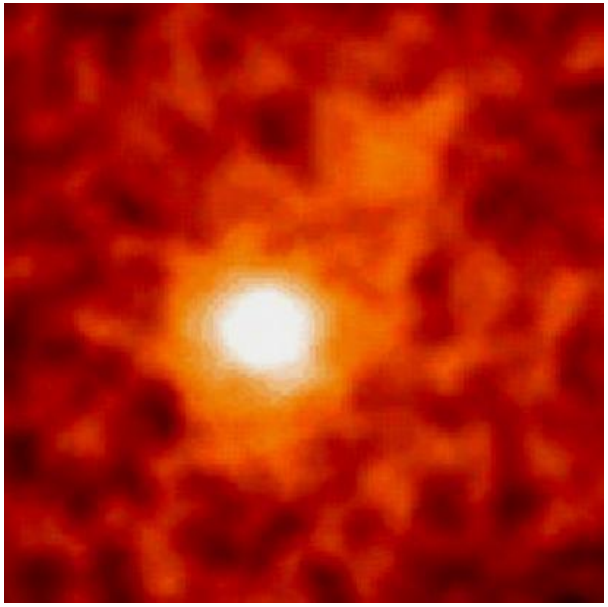

Quasar
3C 279
(OVV)

# Images de 4 équipes indépendantes pour le 11 avril 2017



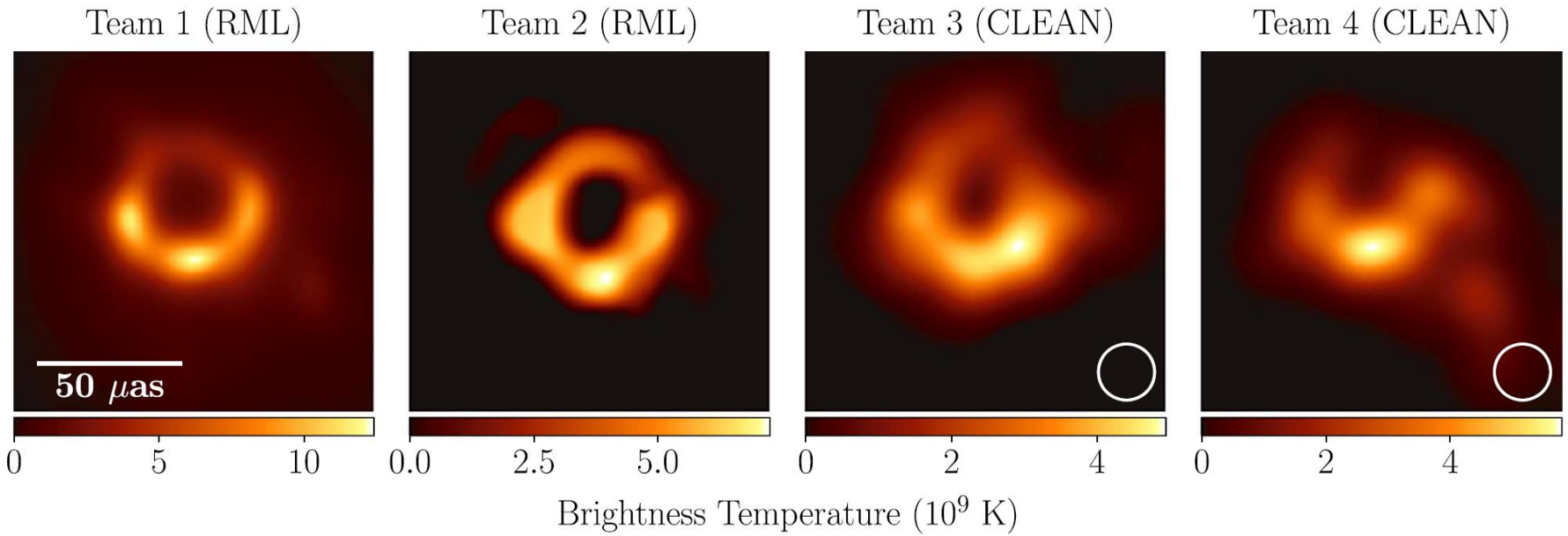


**Figure 4.** The first EHT images of M87, blindly reconstructed by four independent imaging teams using an early, engineering release of data from the April 11 observations. These images all used a single polarization (LCP) rather than Stokes *I*, which is used in the remainder of this Letter. Images from Teams 1 and 2 used RML methods (no restoring beam); images from Teams 3 and 4 used CLEAN (restored with a circular 20 $\mu$as beam, shown in the lower right). The images all show similar morphology, although the reconstructions show significant differences in brightness temperature because of different assumptions regarding the total compact flux density (see Table 2) and because restoring beams are applied only to CLEAN images.

Article # 4

# Observations du trou noir supermassif de M87

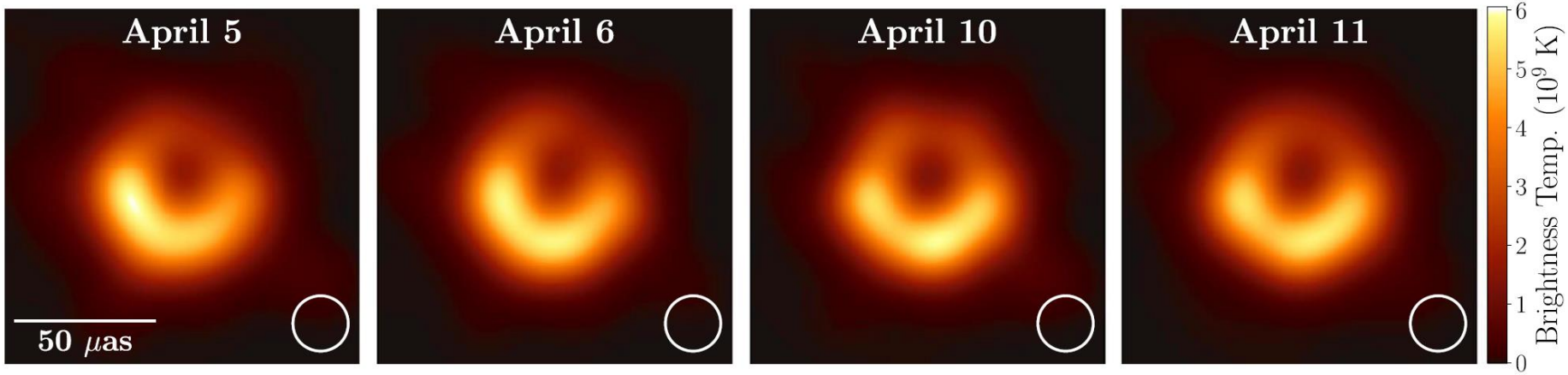


**Figure 15.** Averages of the three fiducial images of M87 for each of the four observed days after restoring each to an equivalent resolution, as in Figure 14. The indicated beam is 20 $\mu$as (i.e., that of DIFMAP, which is always the largest of the three individual beams).

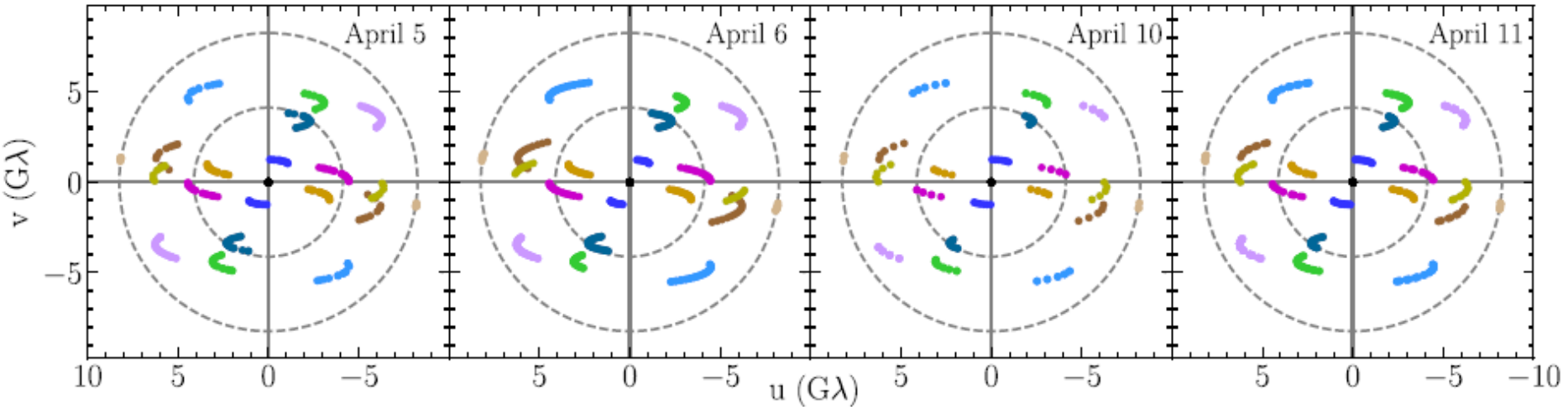

# Variabilité à court terme (1 et 5 jours)



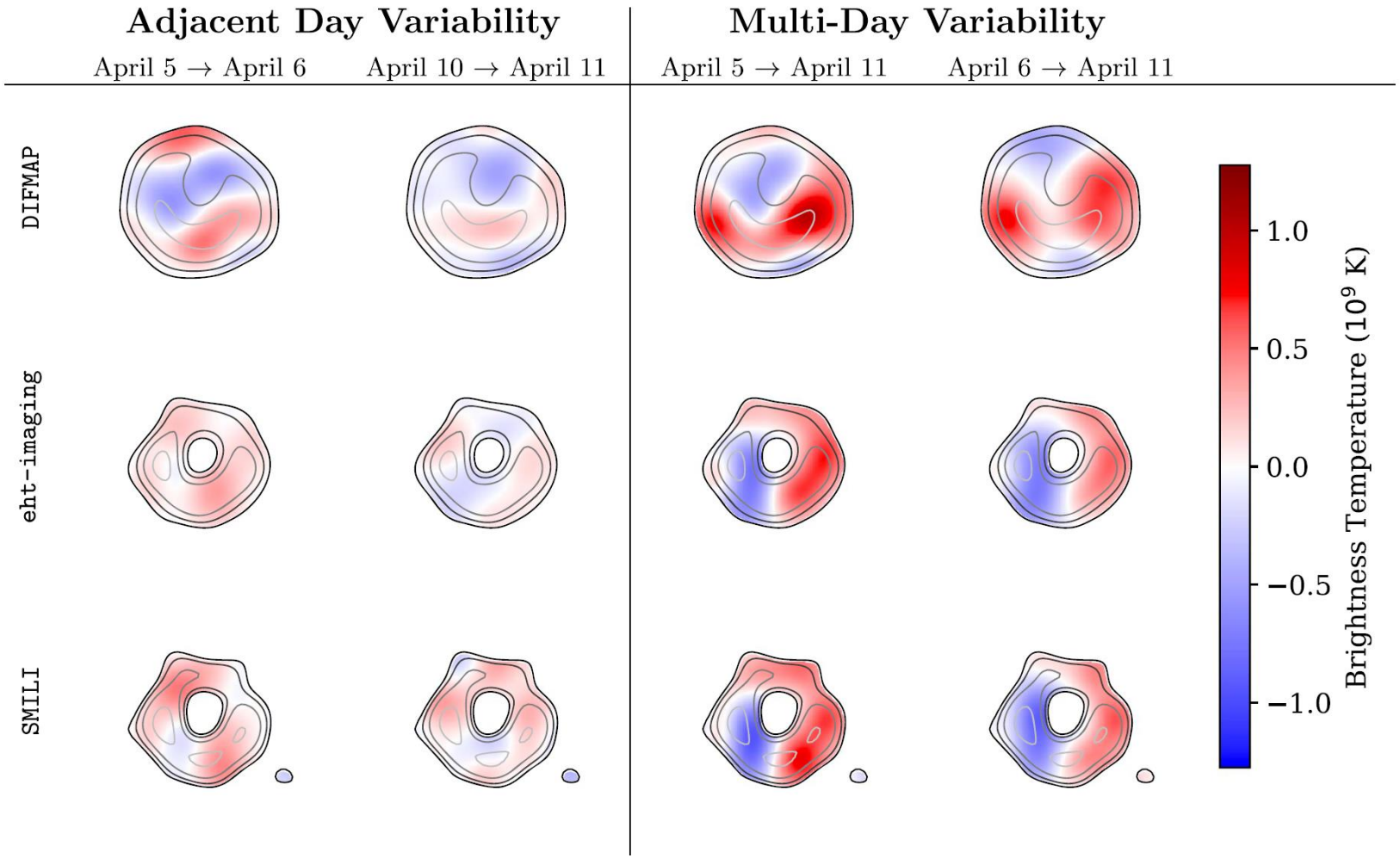


**Figure 33.** Variations seen in reconstructed images between days. Each row shows the beam-convolved difference of the aligned mean images from the Top Set of the corresponding parameter survey. All images are shown using the same color scale. Positive values (red) indicate an increase in brightness at the later date, and negative values (blue) indicate a decrease in brightness at the later date.

Article # 4

# Comparaison entre observation et théorie



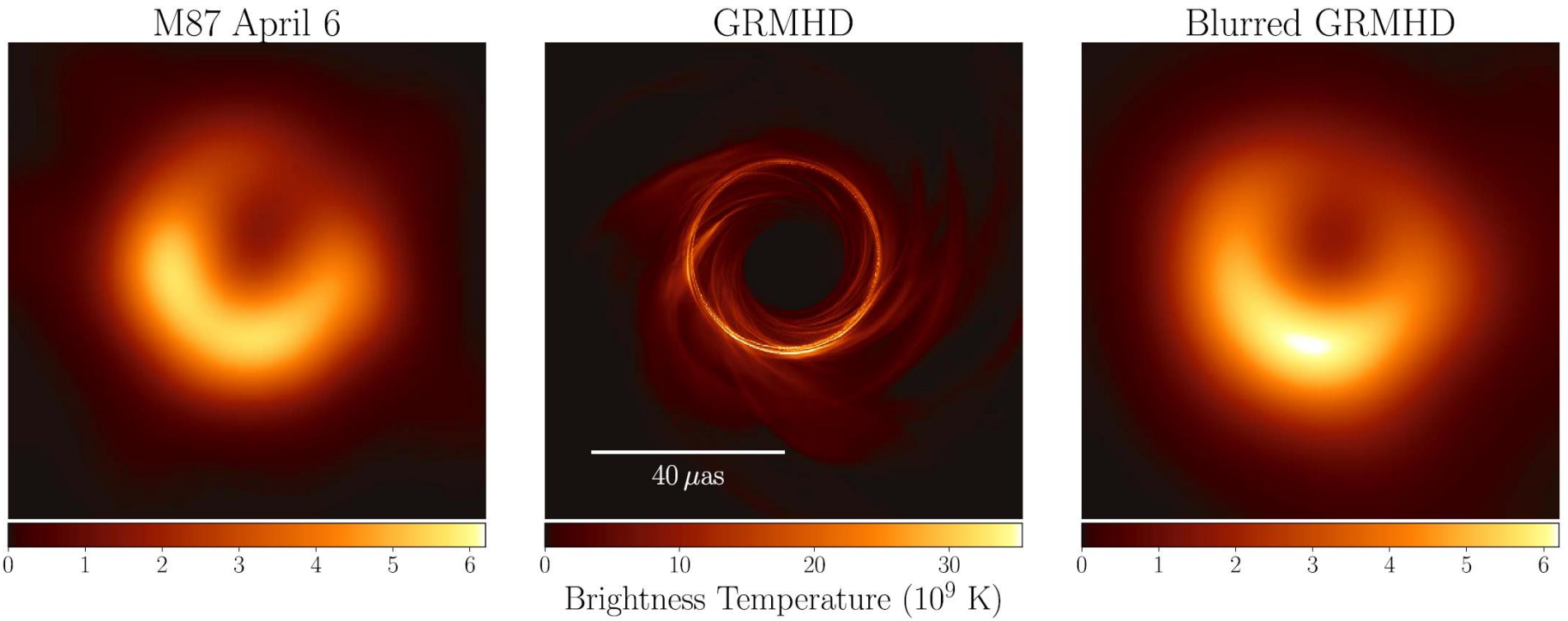


**Figure 1.** Left panel: an EHT2017 image of M87 from Paper IV of this series (see their Figure 15). Middle panel: a simulated image based on a GRMHD model. Right panel: the model image convolved with a 20 $\mu$as FWHM Gaussian beam. Although the most evident features of the model and data are similar, fine features in the model are not resolved by EHT.

Article # 5

# Effets du moment angulaire sur l'asymétrie de l'anneau



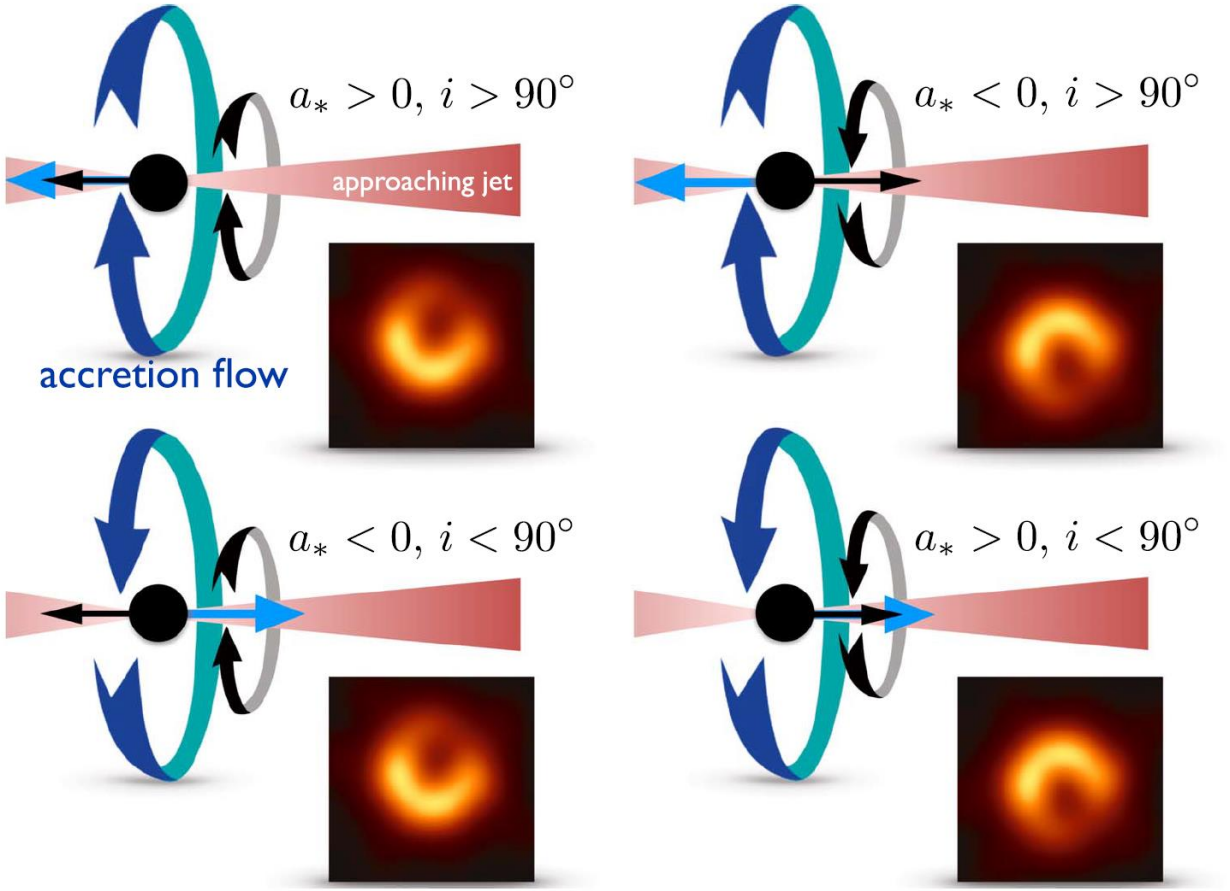


**Figure 5.** Illustration of the effect of black hole and disk angular momentum on ring asymmetry. The asymmetry is produced primarily by Doppler beaming: the bright region corresponds to the approaching side. In GRMHD models that fit the data comparatively well, the asymmetry arises in emission generated in the funnel wall. The sense of rotation of both the jet and funnel wall are controlled by the black hole spin. If the black hole spin axis is aligned with the large-scale jet, which points to the right, then the asymmetry implies that the black hole spin is pointing away from Earth (rotation of the black hole is clockwise as viewed from Earth). The blue ribbon arrow shows the sense of disk rotation, and the black ribbon arrow shows black hole spin. Inclination $i$ is defined as the angle between the disk angular momentum vector and the line of sight.

Article # 5

# Paramètres estimés à partir des images du EHT

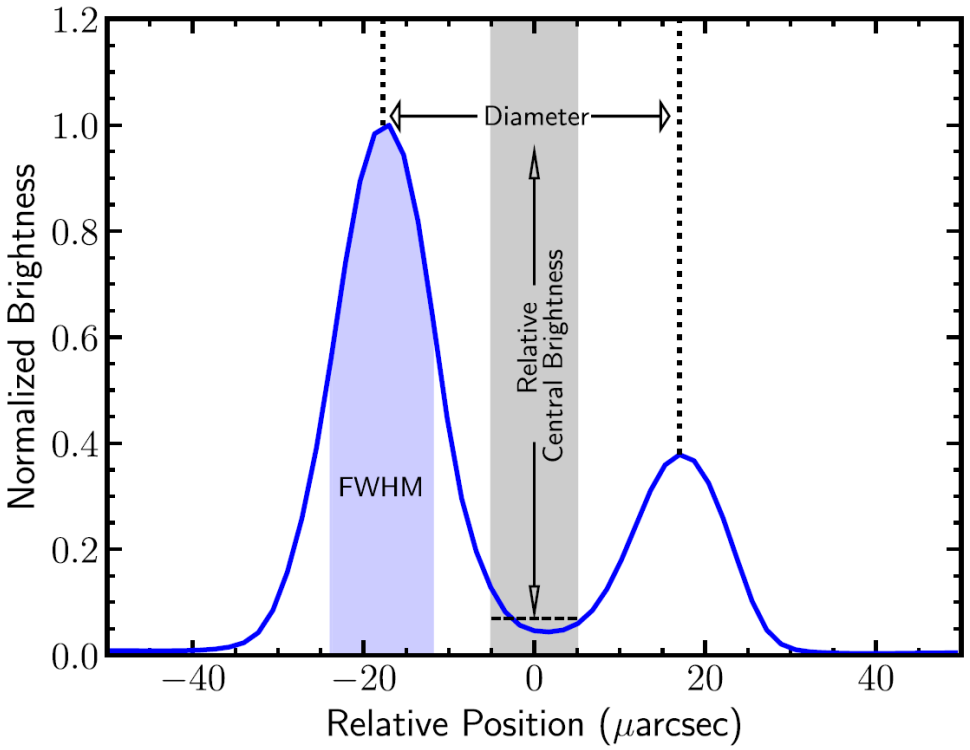


**Figure 14.** A sample image cross section showing the definitions of the image domain measures that we use in identifying and comparing features in the images (see Section 7).

Article # 6

# Masse du trou noir = 6.5 milliards de soleils

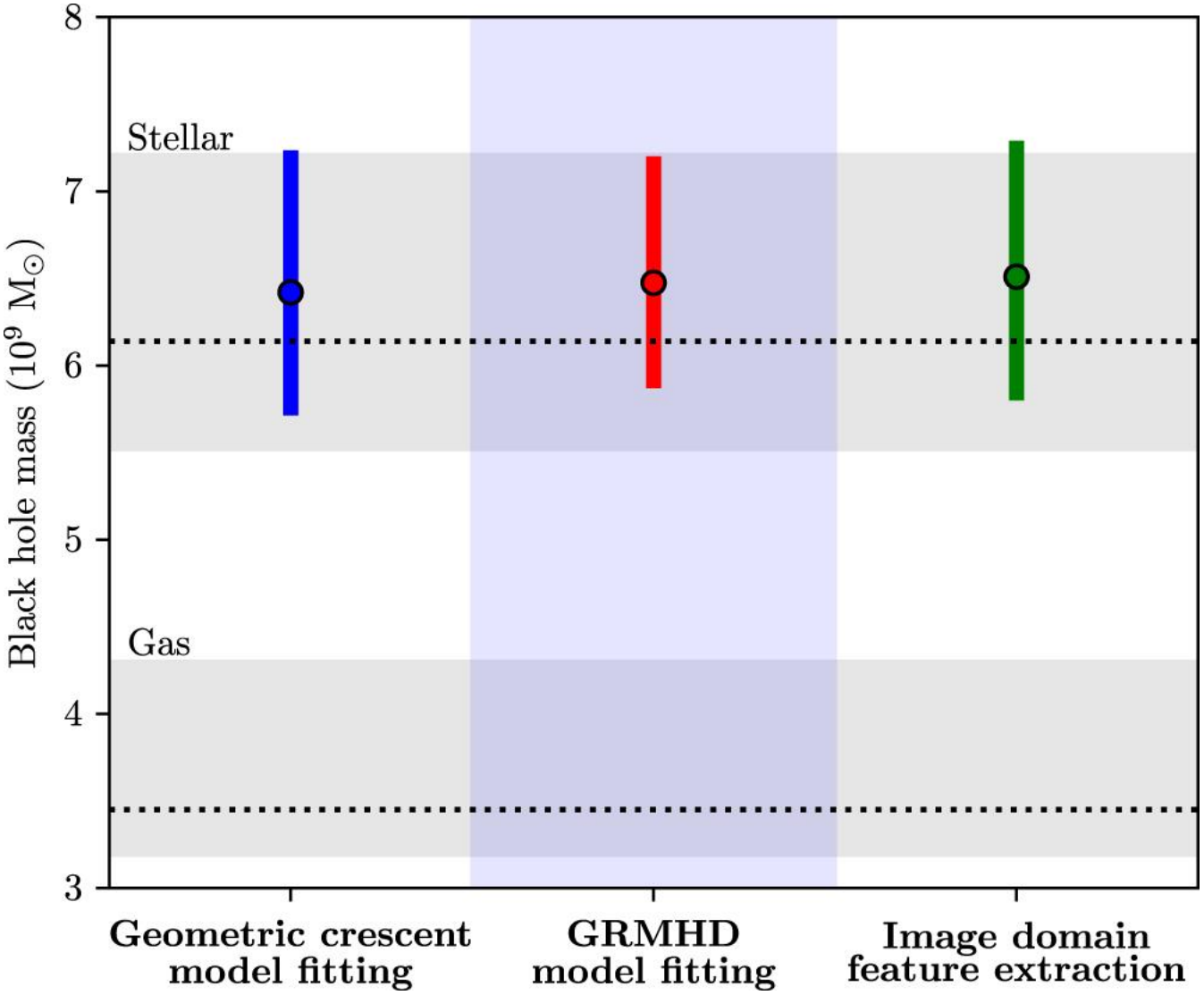


Article # 6, Figure 19

Katie Bouman, M.I.T., coqueluche des médias sociaux, était en charge du traitement des images

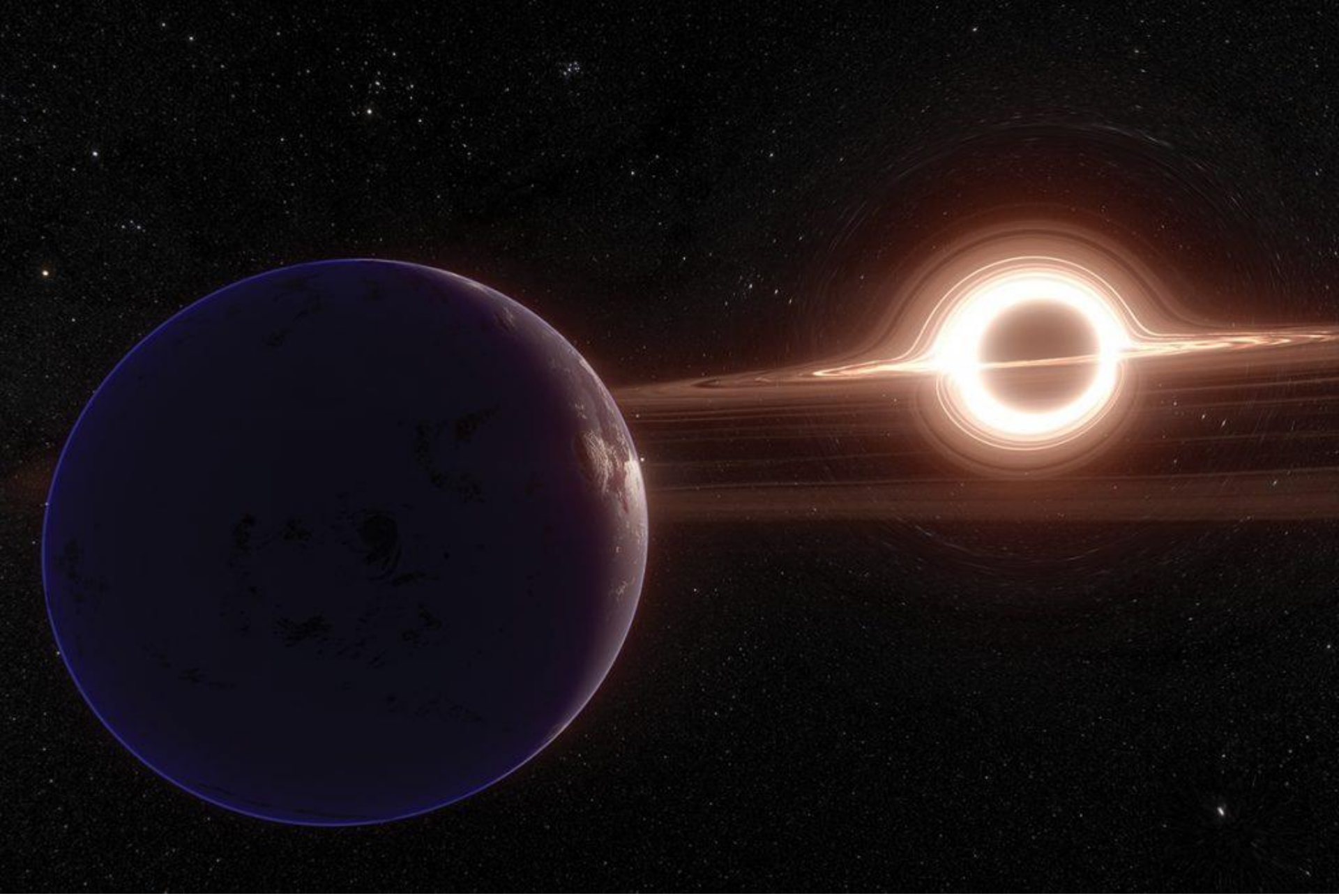

Simulation par ordinateur montrant un trou noir entouré d'un disque d'accrétion. La gravité agit comme une lentille, en incurvant les rayons lumineux émis à l'arrière-plan. Film « Interstellaire ».